JOURNAL OF BACTERIOLOGY, Dec. 2010, p. 6116–6125 Vol. 192, No. 23
0021-9193/10/$12.00 doi:10.1128/JB.00783-10

Evidence from Artificial Septal Targeting and Site-Directed Mutagenesis that Residues in the Extracytoplasmic β Domain of DivIB Mediate Its Interaction with the Divisomal Transpeptidase PBP 2B▽†

Susan L. Rowland,[2]‡ Kimberly D. Wadsworth,[1]‡§ Scott A. Robson,[3]¶
Carine Robichon,[4] Jon Beckwith,[5] and Glenn F. King[1,2]*

Institute for Molecular Bioscience[1] and School of Chemistry and Molecular Biosciences,[2] The University of Queensland, Saint Lucia, Queensland 4072, Australia; Department of Molecular, Microbial and Structural Biology, University of Connecticut Health Center, 263 Farmington Avenue, Farmington, Connecticut 06030[3]; New England Biolabs, Gene Expression Division, 240 County Road, Ipswich, Massachusetts 01938[4]; and Department of Microbiology and Molecular Genetics, Harvard Medical School, 200 Longwood Avenue, Boston, Massachusetts 02115[5]

Received 5 July 2010/Accepted 14 September 2010

Bacterial cytokinesis is achieved through the coordinated action of a multiprotein complex known as the divisome. The *Escherichia coli* divisome is comprised of at least 10 essential proteins whose individual functions are mostly unknown. Most divisomal proteins have multiple binding partners, making it difficult to pinpoint epitopes that mediate pairwise interactions between these proteins. We recently introduced an artificial septal targeting approach that allows the interaction between pairs of proteins to be studied *in vivo* without the complications introduced by other interacting proteins (C. Robichon, G. F. King, N. W. Goehring, and J. Beckwith, J. Bacteriol. 190:6048–6059, 2008). We have used this approach to perform a molecular dissection of the interaction between *Bacillus subtilis* DivIB and the divisomal transpeptidase PBP 2B, and we demonstrate that this interaction is mediated exclusively through the extracytoplasmic domains of these proteins. Artificial septal targeting in combination with mutagenesis experiments revealed that the C-terminal region of the β domain of DivIB is critical for its interaction with PBP 2B. These findings are consistent with previously defined loss-of-function point mutations in DivIB as well as the recent demonstration that the β domain of DivIB mediates its interaction with the FtsL-DivIC heterodimer. These new results have allowed us to construct a model of the DivIB/PBP 2B/FtsL/DivIC quaternary complex that strongly implicates DivIB, FtsL, and DivIC in modulating the transpeptidase activity of PBP 2B.

Bacterial cytokinesis is a highly coordinated process that is carried out by a multiprotein complex known as the divisome (9, 11, 37, 39). In *Escherichia coli*, there are at least 10 essential divisomal proteins that carry out the division process. Divisome formation is initiated at the incipient division site by the recruitment of the FtsZ ring (1) which provides a molecular scaffold onto which the other divisional proteins are subsequently loaded (24, 33) (Fig. 1). In *E. coli*, the first proteins to load after FtsZ are a group of predominantly cytoplasmic proteins (FtsA, ZapA, and ZipA) that stabilize nascent FtsZ protofilaments and tether them to the membrane. The stabilized Z-ring then acts as a platform for recruitment of the remaining essential divisomal proteins, which are all single- or multipass membrane proteins (i.e., FtsE/FtsX, FtsK, FtsQ, FtsB, FtsL, FtsW, FtsI, and FtsN). With the exception of FtsI, a transpeptidase that cross-links septal murein, the biochemical function of these proteins is unknown.

Divisomal protein recruitment in both *Bacillus subtilis* and *E. coli* occurs in a stepwise manner. For example, for FtsQ to be recruited to the *E. coli* divisome, all of the proteins upstream from it in the hierarchical recruitment pathway shown in Fig. 1A must already be present at the septum. However, this pathway is not completely linear; some proteins appear to form subcomplexes prior to their recruitment to the divisome, such as the ternary complex formed between *E. coli* FtsQ, FtsB, and FtsL (2, 12, 14, 15). The situation in *B. subtilis* is more complex and less well understood. For example, *B. subtilis* DivIB, DivIC, FtsL, and PBP 2B appear to be recruited to the septum as an interdependent group late in the cell cycle (10) (Fig. 1B). To further complicate matters, once these individual proteins or subcomplexes have been recruited to the divisome, they engage in a complex network of protein-protein interactions with other divisomal proteins (7, 8, 18, 23).

The plethora of protein-protein interactions at the bacterial divisome makes it difficult to decipher which molecular epitopes on individual proteins mediate their interaction with other divisomal proteins. Thus, we recently introduced an ar-

* Corresponding author. Mailing address: Institute for Molecular Bioscience, The University of Queensland, 306 Carmody Road, St. Lucia, QLD 4072, Australia. Phone: 61 7 3346-2025. Fax: 61 7 3346-2021. E-mail: glenn.king@imb.uq.edu.au.

‡ S.L.R. and K.D.W. contributed equally to this work.

§ Present address: Department of Biochemistry, Molecular Biology and Biophysics, University of Minnesota, 321 Church St., Minneapolis, MN 55455.

¶ Present address: Department of Biological Chemistry and Molecular Pharmacology, Harvard Medical School, 240 Longwood Avenue, Boston, MA 02115.

† Supplemental material for this article may be found at http://jb.asm.org/.

▽ Published ahead of print on 24 September 2010.

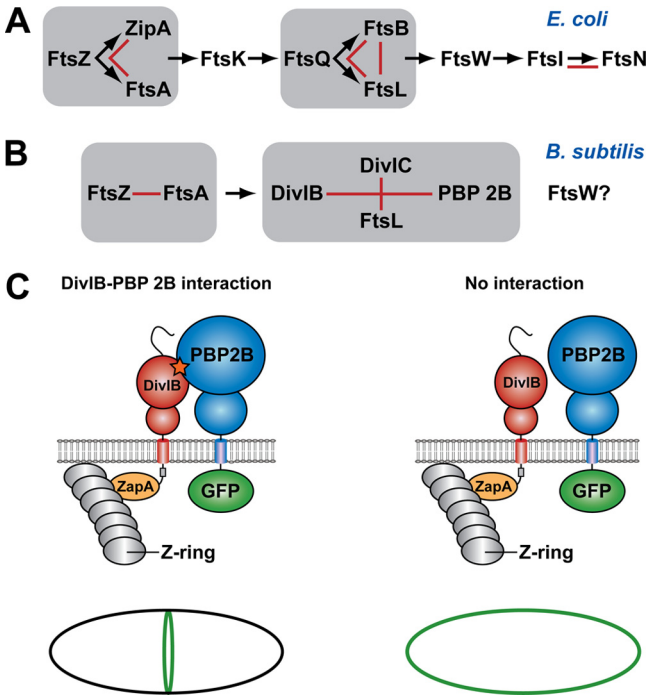

FIG. 1. Schema showing the hierarchical pathway of divisome assembly in *E. coli* and *B. subtilis* (adapted from reference 30). For a protein to be recruited to the divisome, all of the proteins upstream from it in the hierarchical recruitment pathway must already be present at the septum. Groups of proteins that form a subcomplex independent of other divisomal proteins, such as the ternary complex formed between *E. coli* FtsQ, FtsB, and FtsL, are highlighted by gray boxes. Red lines denote pairwise protein-protein interactions that have been experimentally demonstrated using genetic and/or biochemical approaches. The question mark indicates that the precise location of FtsW in the divisome assembly pathway in *B. subtilis* is currently unknown. (C) Possible outcomes of a heterologous septal targeting experiment in *E. coli* in which ZapA-DivIB is employed as the bait and GFP-PBP 2B is the prey. A direct interaction between DivIB and PBP 2B should result in a fluorescent ring at midcell (or a pair of dots when viewed in cross-section) due the recruitment of GFP-PBP 2B to the divisome (left panel). In contrast, a halo of fluorescence should be visible around the cell periphery due to the membrane-bound GFP-PBP 2B if there is no interaction between these two proteins (right panel).

tificial septal targeting (AST) technique that allowed us to examine interactions between pairs of interacting *B. subtilis* divisomal proteins in *E. coli* (30). This technique involves artificially targeting one of the *B. subtilis* proteins (the "bait") to the *E. coli* divisome by fusing it to *E. coli* ZapA and then using fluorescence microscopy to determine whether it can recruit to the septum a green fluorescent protein (GFP) fusion to a putative interacting partner (the "prey") (Fig. 1C). The primary advantage of the AST technique is that it allows direct assessment of the interaction between two *B. subtilis* divisomal proteins without interference from other members of the divisome.

We previously used AST to demonstrate a direct interaction between *B. subtilis* FtsL and DivIC and between DivIB and PBP 2B (30). The latter finding is consistent with the observation from bacterial two-hybrid studies that *B. subtilis* DivIB interacts directly with both PBP 2B and FtsL (5) and that the *E. coli* orthologs of these proteins (FtsI and FtsQ, respectively) also interact strongly (18). The extracellular domain of DivIB is divided into three subdomains, termed α, β, and γ (31). It was recently shown using a combination of nuclear magnetic resonance (NMR) spectroscopy and small-angle X-ray scattering (SAXS) that the concave face of the DivIB β domain makes direct contact with the C-terminal head of the FtsL-DivIC heterodimeric coiled coil (25), forming a stabilizing "cap" for these two intrinsically unstable proteins (32). In contrast, the α and γ regions of DivIB are not critical for formation of the DivIB/FtsL/DivIC ternary complex (25).

The FtsQ/DivIB-FtsI/PBP 2B interaction appears to be widely conserved in both Gram-negative and Gram-positive bacteria, and therefore we decided to investigate the molecular details of this evolutionarily conserved interaction. By using a combination of AST and site-directed mutagenesis, we show that DivIB and PBP 2B interact exclusively through their extracytoplasmic regions and that this interaction is mediated by residues near the C terminus of DivIB. In combination with the results of previous studies, these new data have allowed us to construct a working model of the DivIB/PBP 2B/FtsL/DivIC complex.

MATERIALS AND METHODS

Plasmid and strain construction. We constructed a series of plasmids in which *zapA* was present as a translational fusion to either full-length *divIB*, or various domain deletions thereof, with a C-terminal Myc3 tag (i.e., ZapA-DivIB$_{Myc3}$). The *divIB* fragments for these plasmids were obtained by PCR amplification from plasmids encoding DivIB domain deletion mutants that we constructed previously (38). PCR products were purified, digested using EcoRI and XbaI, and ligated into plasmid pCR27 (30) to generate Myc3-tagged DivIB constructs. The resultant plasmids were digested using EcoRI and HindIII; then the desired fragments were gel purified (QIAquick Gel Extraction Kit; Qiagen, CA) and ligated into plasmid pMDG1 to generate N-terminal ZapA tags on the construct. Expression of the *zapA-divIB*$_{Myc3}$ fusions is isopropyl-β-D-thiogalactopyranoside (IPTG) inducible in the pMDG1-based plasmids. These plasmids (pKDW38 through pKDW40, pKDW42, pKDW44, pKDW48, pKDW49, and pSLR117 through pSLR119) were sequenced, and then strain CR362 was transformed with the plasmids. Cells were plated on NZY (N-Z amine, yeast extract) plates supplemented with agar, 100 μg/ml spectinomycin (Spc), and 25 μg/ml ampicillin (Amp) for selection. Point mutations were introduced into *divIB* for incorporation at the *amyE* chromosomal locus of *B. subtilis* as described previously, using pSAR50 as a template and pDG364 as the cloning vector (31).

DivIB mutant strain construction. Construction of the *divIB* null strain RSA8 (Δ*divIB*::*cat*::*ermC*) and RSA8-derived strains carrying an inducible copy of *divIB* at the *amyE* locus has been described previously (31). Strains produced for this study are numbered RSA11 through RSA19, RSA21, RSA22, RSA24 through RSA28, RSA30, and RSA31. Table 1 provides a summary of all strains and plasmids used in this study while Table S1 in the supplemental material provides a list of templates and primers.

Bacterial growth conditions. For microscopy and Western blot analyses, *E. coli* strains were grown in LB medium at 37°C overnight (~16 h) with shaking. Cultures were then diluted 1:100 with LB medium and grown at 30°C with shaking to an optical density at 600 nm (OD$_{600}$) of ~0.3. Cells were then induced with 20 or 50 μM IPTG for 30 to 60 min. *B. subtilis* temperature sensitivity was tested by streaking strains on duplicate plates grown at 30°C and 48°C and monitoring colony growth at 16 h and 24 h.

Fluorescence microscopy. Cells were grown as described above and viewed both fixed and unfixed. Fixed cells were used for all figures. Cells were fixed by adding 47 μl of 16% paraformaldehyde, 0.5 μl of 25% glutaraldehyde, and 10 μl of 1 M $NaPO_4$ (pH 7.5) to each 250-μl cell culture sample. These samples were incubated at room temperature for 15 min and then on ice for at least 40 min. The samples were pelleted by centrifugation (3 min at 17,000 × *g*). A 250-μl aliquot of saline (0.84% NaCl) was added, and the sample was centrifuged for 3 min. This step was repeated, and the cell pellet was resuspended in approximately 50 μl of saline. Fluorescence micrographs were obtained using a 100×

TABLE 1. Plasmids and strains

Plasmid or strain	Genotype[a]	Source or reference
Plasmids		
pDSW204	IPTG regulated promoter, pBR322 origin; Amp	40
pDSW207	pDSW204-*gfp*-MCS (fusion vector)	40
pCR27	pDSW207 containing *myc3*	30
pMDG1	pNG162 containing *zapA-malF*$_{cyto}$-*ftsB*	M. D. Gonzalez
pNG162	IPTG regulated promoter (pDSW204), pSC101 origin; Spc	12
pKDW38	pNG162 containing *zapA-malF*$_{cyto}$-$C_{IB}T_{IB}$-*myc3*; Spc	This study
pKDW39	pNG162 containing *zapA-malF*$_{cyto}$-$C_{IB}T_{IB}\alpha_{IB}\beta_{IB}\gamma_{IB}$-*myc3*; Spc	This study
pKDW40	pNG162 containing *zapA-malF*$_{cyto}$-$C_{IB}T_{IB}\alpha_{IB}$-*myc3*; Spc	This study
pKDW42	pNG162 containing *zapA-malF*$_{cyto}$-$C_{IB}T_{IB}\beta_{IB}\gamma_{IB}$-*myc3*; Spc	This study
pKDW48	pNG162 containing *zapA-malF*$_{cyto}$-$C_{IB}T_{IB}\alpha_{IB}\beta_{IB}$-*myc3*; Spc	This study
pKDW49	pNG162 containing *zapA-malF*$_{cyto}$-$C_{TR}T_{TR}\alpha_{IB}\beta_{IB}\gamma_{IB}$-*myc3*; Spc	This study
pSG1729	*B. subtilis amyE* integration vector; P_{xyl} *bla spc*	21
pKDW44	pSG1729 containing *E. coli FtsQ*; P_{xyl} *bla spc*	This study
Strains		
E. coli		
JOE309	MC4100 *ara*$^+$	3
CR362	JOE309 Δ(λ*attL-lom*)::*bla lacI*^{q}/pDSW204-*gfp-pbpB-myc3*	30
CR363	JOE309 Δ(λ*attL-lom*)::*bla lacI*^{q}/pDSW204-*gfp-pbpB*	30
B. subtilis		
SU5 (or 168)	*trpC2*	Laboratory collection
RSA8	*trpC2 divIB*::*cat*::*ermC*	31
RSA9	*trpC2 divIB*::*cat*::*ermC amyE*::*divIB cat*	31
RSA24	*trpC2 divIB*::*cat*::*ermC amyE*::*divIB(E122A) cat*	This study
RSA16	*trpC2 divIB*::*cat*::*ermC amyE*::*divIB(L139A) cat*	This study
RSA18	*trpC2 divIB*::*cat*::*ermC amyE*::*divIB(N141A) cat*	This study
RSA26	*trpC2 divIB*::*cat*::*ermC amyE*::*divIB(E187A) cat*	This study
RSA19	*trpC2 divIB*::*cat*::*ermC amyE*::*divIB(Y203A) cat*	This study
RSA21	*trpC2 divIB*::*cat*::*ermC amyE*::*divIB(N205A) cat*	This study
RSA22	*trpC2 divIB*::*cat*::*ermC amyE*::*divIB(D206A) cat*	This study
RSA30	*trpC2 divIB*::*cat*::*ermC amyE*::*divIB(Y224A) cat*	31
RSA31	*trpC2 divIB*::*cat*::*ermC amyE*::*divIB(P225A) cat*	31
RSA28	*trpC2 divIB*::*cat*::*ermC amyE*::*divIB(Y246A) cat*	This study

[a] In the plasmid notation, the subscripts IB and TR indicate that the domains are from *B. subtilis* DivIB and *E. coli* TolR, respectively, and C and T refer to the cytoplasmic and transmembrane domains, respectively. The three extracytoplasmic domains of DivIB are referred to as α, β, and γ (31). MCS, multiple cloning site; cyto, cytoplasmic region.

objective on an Olympus BX40 microscope equipped with a MagnaFire digital camera (Optronics International, Chelmsford, MA).

Western blot analyses. For Western blot analyses of *E. coli* strains, a 1-ml cell culture was harvested by centrifugation, and the cell pellet was resuspended in 40 μl of lysis buffer (50 mM NaCl, 50 mM Tris, 1 mM EDTA, pH 8.0) and 40 μl of 2× SDS-PAGE loading buffer. Samples were boiled at 100°C and then electrophoresed on a 10% SDS-PAGE gel. Following electrophoresis, gels were electroblotted onto a Hybond-LFP polyvinylidene difluoride (PVDF) membrane (GE Healthcare UK Limited, Buckinghamshire, United Kingdom). For detection of Myc-tagged DivIB and PBP 2B, immunoblots were probed using a rabbit anti-c-Myc primary antibody (Sigma-Aldrich), followed by a Cy5-conjugated secondary antibody (GE Healthcare UK Limited). Immunoblots were visualized dry using a Typhoon 8600 Imager (Amersham Pharmacia Biotech).

RESULTS

PBP 2B and DivIB interact through their extracytoplasmic regions. We used AST to determine which regions of DivIB are responsible for its interaction with PBP 2B. In this approach, *B. subtilis* DivIB is targeted to the septum by fusion to *E. coli* ZapA. The ZapA-DivIB fusion is then used as a bait to attract the prey, in this case a fusion of the PBP 2B protein to GFP. A DivIB-PBP 2B interaction should lead to a ring of fluorescence at midcell due to localization of GFP-PBP 2B to the *E. coli* septum (Fig. 1C, left panel). Alternatively, if the two proteins do not interact, one should observe a halo of fluorescence around the cell periphery since the GFP-PBP 2B fusion will be membrane bound but not localized to the septum (Fig. 1C, right panel). We reasoned that by varying the region of DivIB that is used as the bait, it should be possible to determine the epitopes on DivIB that mediate its interaction with PBP 2B.

We previously showed that neither DivIB nor PBP 2B localizes to division septa in *E. coli* and that neither protein can complement its respective *E. coli* null strain (i.e., ablation of *ftsQ* and *ftsI*, respectively) (30). However, a ZapA-DivIB fusion protein can recruit GFP-PBP 2B to division septa in *E. coli* (30). Thus, in the experiments shown in Fig. 2, localization of GFP-PBP 2B to midcell is indicative of an interaction with ZapA-DivIB.

As shown previously, expression of full-length ZapA-DivIB leads to recruitment of GFP-PBP 2B to division septa in *E. coli*, as judged by the presence of fluorescent dot(s) or stripes at midcell (Fig. 2A). While the molecular epitopes responsible for septal localization of PBP 2B have not yet been determined, the orthologous *E. coli* protein, FtsI (also known as PBP3), contains a strong septal localization signal within its single-pass transmembrane (TM) domain (28, 41, 42). Since DivIB also contains a septal localization determinant within its

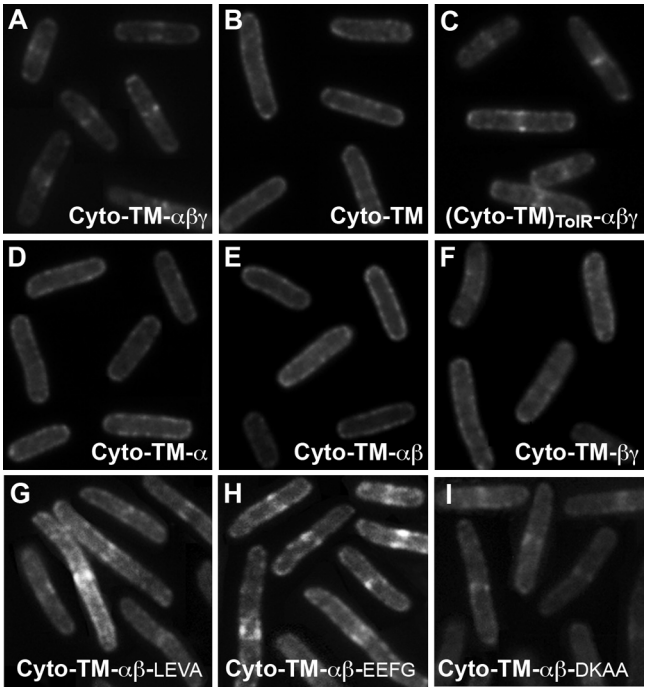

FIG. 2. Fluorescence micrographs resulting from heterologous septal targeting experiments in *E. coli* in which the prey was GFP-PBP 2B and the bait was *E. coli* ZapA fused to either full-length DivIB (A) or one of the following: the Cyto-TM region only of DivIB (B), the entire extracytoplasmic region of *B. subtilis* DivIB fused to the Cyto-TM region of *E. coli* TolR (C), a truncated version of DivIB missing the C-terminal β domain and γ tail (D), a truncated version of DivIB missing the C-terminal γ tail (E), or a DivIB mutant in which the extracytoplasmic α domain has been excised (F). Panels G to I show the GFP-PBP 2B localization patterns obtained when the β domain in the Cyto-TM-αβ construct was extended by 16 residues (Cyto-TM-αβ-LEVA), 23 residues (Cyto-TM-αβ-EEFG), or 29 residues (Cyto-TM-αβ-DKAA). Septal localization of GFP-PBP 2B in panels A and C and G to I is indicated by fluorescent stripes or dots at midcell.

TM domain (38), we wondered whether the DivIB-PBP 2B interaction might be mediated entirely through the TM regions of these proteins. However, as shown in Fig. 2B, a construct consisting of ZapA fused to only the cytoplasmic (Cyto) and TM regions of DivIB [ZapA-$(Cyto\text{-}TM)_{DivIB}$] was incapable of recruiting GFP-PBP 2B to division septa, as indicated by the halo of fluorescence around the cell periphery and the absence of midcell localization. We therefore conclude that either these proteins do not interact through their TM regions, or, if they do, the interaction affinity is too weak to allow significant recruitment of PBP 2B to the division site.

The corollary of the above conclusion is that the major sites of interaction between these proteins must be their extracytoplasmic regions. To confirm this, we constructed a protein consisting of ZapA fused to a DivIB in which $(Cyto\text{-}TM)_{DivIB}$ regions were replaced by the corresponding regions of the unrelated *E. coli* protein TolR, yielding ZapA-$(Cyto\text{-}TM)_{TolR}$-αβγ. As shown in Fig. 2C, ZapA-$(Cyto\text{-}TM)_{TolR}$-αβγ was able to recruit PBP 2B to midcell, indicating that the extracytoplasmic region of DivIB must contain the primary molecular epitopes that mediate its interaction with PBP 2B.

The extracytoplasmic region of DivIB is comprised of two autonomously folded N-terminal domains, termed α and β, and an unstructured C-terminal segment referred to as γ (31) (Fig. 3). Although the unstructured γ "domain" in *B. subtilis* DivIB might be as short as ~20 residues (see discussion below), this region comprises >60 residues in some species. We have chosen to refer to this region as the γ tail to be consistent with recent work on *Streptococcus pneumoniae* DivIB (25) and to highlight the fact that this region is unstructured, at least in the absence of other divisomal proteins (25, 31).

In *B. subtilis* DivIB, the three extracytoplasmic regions were originally defined as residues 51 to 122 (α), 123 to 228 (β), and 229 to 263 (γ) (31, 38). As will be discussed in more detail below, there is some debate about the exact boundary between the β and γ domains in DivIB (25, 36), but we used the originally defined domain boundaries for initial studies. In these experiments, we made a fusion of ZapA to the cytoplasmic and TM regions of DivIB and then added various combinations of DivIB extracellular domains to determine which domains were capable of recruiting GFP-PBP 2B.

As shown in Fig. 2D, the α domain alone (Cyto-TM-α) is insufficient to support an interaction with PBP 2B. Constructs comprising either the α and β domains together (Fig. 2E) or the β and γ domains together (Fig. 2F) were also incapable of recruiting PBP 2B to division septa, as evidenced by the halo of fluorescence around the cell periphery and the absence of midcell localization. Previous work suggests that the absence of PBP 2B recruitment by these ZapA-DivIB fusions was not due to misfolding, low levels of expression, and/or instability of the fusion proteins (31, 38). The separated α and β domains of DivIB used in this study (i.e., residues 51 to 122 of *B. subtilis* DivIB [$DivIB_{51\text{-}122}$] and $DivIB_{123\text{-}228}$, respectively) were previously shown to be functional (38), and, as demonstrated by Western blotting (Fig. 4), all of the ZapA-DivIB fusion proteins were expressed in *E. coli* at readily detectable levels. Although the anti-Myc antibody we used clearly produces some cross-reactivity with endogenous *E. coli* proteins, it is clear that the truncated DivIB proteins that did not recruit PBP 2B (Fig. 4, lanes 2, 4, 5, and 6) are produced in significant quantities, and some are expressed at significantly higher levels than DivIB constructs that do localize PBP 2B (Fig. 4, compare lanes 3 and 4). Thus, we conclude that these truncation mutants do not recruit PBP 2B to the septum because they are missing epitopes that are required to form a stable association.

The C-terminal region of the DivIB β domain is critical for interaction with PBP 2B. It is tempting to conclude from the results presented above that no single extracytoplasmic domain of DivIB contains a protein-protein interaction epitope that is sufficient by itself to support an interaction with PBP 2B. Rather, these results suggest that the extracytoplasmic region of DivIB makes a multidentate interaction with the extracytoplasmic region of PBP 2B and that the combined protein-protein interaction epitopes provide sufficient affinity to recruit PBP 2B to division septa. However, an alternative explanation of these results is that the boundaries between the β and γ regions of DivIB were not correctly defined in the initial constructs.

The recently determined crystal structures of *E. coli* and *Yersinia enterocolitica* FtsQ (the Gram-negative ortholog of DivIB) indicate that the β domain might be slightly longer than originally defined by limited proteolysis of *B. subtilis* and

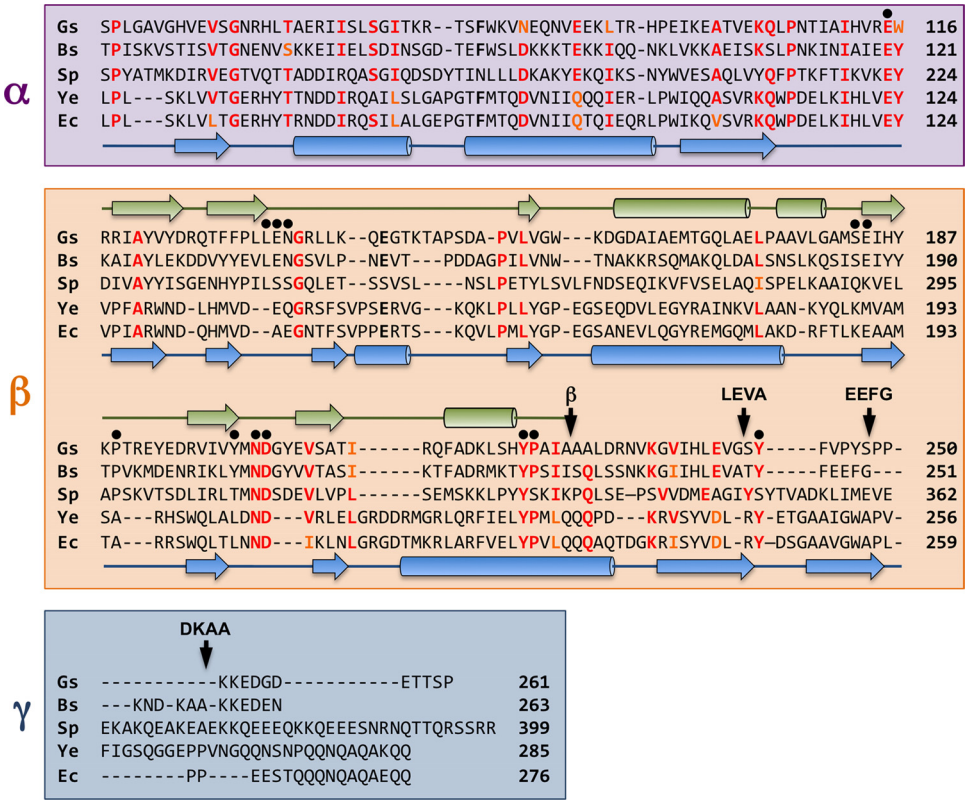

FIG. 3. Structure-based alignment of the amino acid sequences of the extracytoplasmic regions of DivIB from *G. stearothermophilus* (Gs), *B. subtilis* (Bs), and *S. pneumoniae* (Sp) and the amino acid sequences of FtsQ from *Y. enterocolitica* (Ys) and *E. coli* (Ec). The α and β domains and γ tail are highlighted in violet, orange, and blue, respectively; see text for a discussion of the exact location of the β/γ boundary. The arrow labeled β indicates the boundary of the DivIB β domain as defined previously (38) while other arrows labeled LEVA, EEFG, and DKAA indicate the boundaries of the extended β domains used for artificial septal targeting. Black dots highlight residues that were mutated in the current study. The secondary structure of *G. stearothermophilus* DivIB as determined from solution NMR studies (31) is shown in green above the sequences, while the secondary structure of *E. coli* FtsQ as determined using X-ray crystallography (36) is shown in blue below the sequences. Residue numbers are indicated at the end of each sequence.

Geobacillus stearothermophilus DivIB proteins (31). More specifically, these crystal structures revealed that the β-sheet defined in the NMR solution structure of *G. stearothermophilus* DivIB comprises two additional C-terminal β-strands in FtsQ (36). The sequence homology between DivIB and FtsQ is extremely poor over this region of the proteins (Fig. 3, sequence alignments), but recent limited proteolysis studies performed on *S. pneumoniae* DivIB support the suggestion from the crystal structures that the DivIB β domain could be 20 to 25 residues longer than we originally proposed (25). Thus, we decided to examine the effect of extending the C-terminal boundary of the β domain.

We made three additional Cyto-TM-αβ constructs in which the C-terminal boundary of the β domain was extended by adding back either 16 residues (Cyto-TM-αβ-LEVA), 23 residues (Cyto-TM-αβ-EEFG), or 29 residues (Cyto-TM-αβ-DKAA) of the native sequence (the name for each construct indicates the last four residues of the construct) (Fig. 3). As shown in Fig. 2G, addition of 16 residues to the C terminus of the original Cyto-TM-αβ construct is sufficient to recruit a significant amount of GFP-PBP 2B to midcell. For experiments with the Cyto-TM-αβ-LEVA construct, we counted 78/122 cells (i.e., 64%) with midcell localizations, which is similar to the level achieved with full-length DivIB (midcell localization in 185/301 cells, i.e., 61.4%). Addition of an additional seven C-terminal residues in the Cyto-TM-αβ-EEFG and 13 residues in the Cyto-TM-αβ-DKAA constructs also produced a wild-type recruitment pattern (compare Fig. 2A, H, and I). The frequency of midcell localization for these two constructs was 68.5% for EEFG (161/235 cells) and 82.4% for DKAA (150/182 cells). This is a higher level of midcell localization than obtained with full-length DivIB Cyto-TM-αβγ (61.4%), which may indicate that the γ tail (which is not present in the extended β-domain constructs) negatively regulates the interaction between DivIB and PBP 2B. In any case, it is clear that extending the C terminus of the β domain to include the DKAA sequence is required for optimal interaction with PBP 2B.

The high level of midcell localization obtained for each of the extended β-domain constructs stands in stark contrast to the frequency of septal localization seen when the original Cyto-TM-αβ construct was used as bait (15/358 cells, or 4.2% septal localization) (Fig. 2E). Thus, these results support the extended C-terminal boundary of the DivIB β domain as proposed by Masson et al. (25), and they indicate that residues at the extreme C-terminal boundary of the β domain (corre-

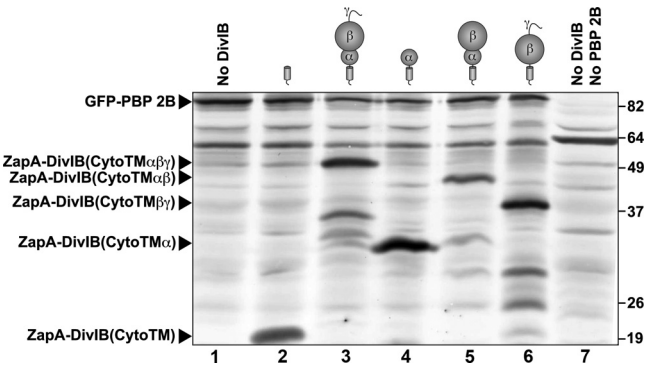

FIG. 4. Western blot obtained by probing *E. coli* cell extracts that expressed various combinations of *B. subtilis* DivIB and PBP 2B with an anti-c-Myc antibody. In all cases, DivIB and PBP 2B were expressed as fusions to the C terminus of *E. coli* ZapA and GFP, respectively. Lane 1, CR362/pMDG1 expressing GFP-PBP $2B_{Myc3}$ and ZapA-FtsB; lane 2, CR362/pKDW38 expressing GFP-PBP $2B_{Myc3}$ and ZapA-DivIB(Cyto-TM_{Myc3}); lane 3, CR362/pKDW39 expressing GFP-PBP $2B_{Myc3}$ and ZapA-DivIB(Cyto-TM-$\alpha\beta\gamma_{Myc3}$); lane 4, CR362/pKDW40 expressing GFP-PBP $2B_{Myc3}$ and ZapA-DivIB(Cyto-TM-α_{Myc3}); lane 5, CR362/pKDW48 expressing GFP-PBP $2B_{Myc3}$ and ZapA-DivIB(Cyto-TM-$\alpha\beta_{Myc3}$); lane 6, CR362/pKDW42 expressing GFP-PBP $2B_{Myc3}$ and ZapA-DivIB(Cyto-TM-$\beta\gamma_{Myc3}$); lane 7, strain CR363 expressing native (i.e., non-Myc-tagged) PBP 2B. The molecular masses of the standards (in kDa) are shown on the right of the blot. The form of DivIB expressed in each cell extract is indicated schematically above each lane of the immunoblot, and the running positions of the ZapA-DivIB fusions are indicated on the left of the blot. The electrophoretic mobilities of all of the fusion proteins were consistent with their predicted molecular masses.

sponding to residues 229 to 257 in *B. subtilis* DivIB) are critical for the interaction of DivIB with PBP 2B. Curiously, residues 229 to 257 are present in the Cyto-TM-βγ construct, which fails to recruit PBP 2B to division septa (Fig. 2F). This indicates that these residues must be (i) present for DivIB to interact with PBP 2B and (ii) presented in an appropriate topological context for the interaction to occur. Based on the crystal structures of the extracytoplasmic domains of *E. coli* and *Y. enterocolitica* FtsQ (36), we estimate that the β domain in full-length DivIB is located about 3 nm from the membrane surface due to the presence of the membrane-proximal α domain. In contrast, in the Cyto-TM-βγ construct, the β domain is located adjacent to the extracellular surface of the cell membrane, where it is presumably incapable of making appropriate interactions with PBP 2B.

Mutagenesis confirms the importance of the C-terminal region of the β domain. The AST studies indicate that the region spanning residues 229 to 257 of *B. subtilis* DivIB is critical for its interaction with PBP 2B. This is consistent with several previous findings which indicate that the C-terminal region of the β domain is critical for DivIB function. Loss of *B. subtilis* DivIB function is caused by (i) G237R and G237E point mutations (17), (ii) a frameshift mutation that results in replacement of the native C terminus with 16 nonnative residues following S233 (17), and (iii) deletion of the C-terminal 31 residues of *B. subtilis* DivIB (i.e., residues S233 to N263) (31). We propose that this loss of function stems from the role of this region in mediating interactions with PBP 2B.

In order to determine whether other regions of the β domain might be critical for DivIB function, we mutated selected residues to Ala and determined whether these mutants could rescue a *divIB* null strain using a previously described complementation assay (31). We mutated 13 surface-exposed residues that are either well conserved across both Gram-negative and Gram-positive bacteria or identical in most Gram-positive species (Fig. 3). Although strongly conserved, L158 and L177 were not mutated; the side chains of these residues are deeply buried in the hydrophobic core of the *G. stearothermophilus* DivIB and *E. coli* FtsQ structures (31, 36). Alanine was used for mutagenesis because it is a small, neutral amino acid that can be accommodated in most types of protein secondary structure, and therefore mutating amino acid residues to alanine is unlikely to perturb the protein fold. Remarkably, virtually all of the mutant DivIB proteins were able to rescue a *divIB* null strain at the nonpermissive growth temperature (Table 2). The only exception was the Y246A mutant, which is also the only mutant that maps to the C-terminal region of the DivIB structure. Cells with this mutation form colonies on plates at the nonpermissive temperature for a *divIB* null strain, but they lyse after 24 h of growth (suggestive of impaired murein synthesis). In addition, these cells were slightly filamentous in liquid culture at the nonpermissive temperature; the average cell length was approximately double that of the wild-type strain but much shorter than that of a *divIB* null strain under the same conditions. We have shown previously that DivIB with a γ-tail deletion localizes to the septum (38). This suggests that the Y246A mutant cannot support normal colony growth because Y246 is a key part of the molecular epitope in the C-terminal region of the β domain that mediates the interaction between DivIB and PBP 2B.

DISCUSSION

Studying divisomal interactions using heterologous septal targeting. The divisome is a macromolecular machine that orchestrates one of the most complex and important subcellular differentiation events in bacteria, namely, partitioning of

TABLE 2. Mutational analysis of DivIB[a]

Strain	Mutation	Source or reference	Growth at 30°C	Growth at 48°C
RSA9	Wild type	31	+	+
RSA24	E122A	This study	+	+
RSA16	L139A	This study	+	+
RSA17	E140A	This study	+	+
RSA18	N141A	This study	+	+
RSA25	S186A	This study	+	+
RSA26	E187A	This study	+	+
RSA27	P192A	This study	+	+
RSA19	Y203A	This study	+	+
RSA21	N205A	This study	+	+
RSA22	D206A	This study	+	+
RSA30	Y224A	31	+	+
RSA31	P225A	31	+	+
RSA28	Y246A	This study	+	+/−[b]

[a] Results of a complementation assay (31) that monitors the ability of mutant *divIB* expressed from an ectopic locus to complement a *divIB* null strain at permissive (30°C) and nonpermissive (48°C) growth temperatures. All strains showed growth (+).

[b] Lysis at 24 h.

the parent bacterium into two daughter cells. Surprisingly, despite years of intensive research, we still know very little about the three-dimensional architecture of the divisome, the specific role of individual divisomal proteins, or how these proteins interact with one another. Thus, our understanding of the mechanism of bacterial cytokinesis remains limited, and this in turn restricts our ability to develop antimicrobial agents that target the bacterial cell division machinery (22).

In the absence of even a low-resolution structure of the bacterial divisome, one of the greatest challenges is to unravel the key protein-protein interactions that are essential for formation of a functional divisome. In this study, we used artificial septal targeting to examine the interaction between DivIB and PBP 2B and showed that this can be a useful approach for dissecting the details of pairwise interactions between divisomal proteins. DivIB is a multidomain protein that comprises a short cytoplasmic domain, a single-pass TM domain, and three extracytoplasmic regions designated α, β, and γ from the N to C terminus (31). We recently showed that septal localization determinants were located in the TM, α, and β/γ domains, and we proposed that these sites represent epitopes that mediate interactions with other divisomal proteins (38). In the current study, we demonstrated that the cytoplasmic and transmembrane domains of DivIB are completely dispensable for interaction with PBP 2B but that this pairwise interaction requires a short stretch of residues near the C terminus of the extracytoplasmic β domain.

Construction of a model of the DivIB/PBP 2B/FtsL/DivIC complex. DivIC, FtsL, DivIB, and PBP 2B are recruited to the *B. subtilis* divisome in an interdependent manner, and it has been proposed that they initially form a quaternary complex away from the division site that is subsequently trafficked to the developing divisome (32). By combining results from the current study with those from a number of recent investigations (14–16, 36, 38), we have developed a working model of the DivIB/PBP 2B/FtsL/DivIC complex.

In this model, we used the crystal structure of the extracytoplasmic region of *E. coli* FtsQ (36) as a proxy for the structure of DivIB since it encompasses more of the extracytoplasmic region of the protein than the solution structure of the isolated β domain of *G. stearothermophilus* DivIB (31). Nevertheless, there is an important caveat. Although the α/β and β/γ domain boundaries for DivIB and FtsQ are likely very similar (25), the limited sequence homology between the extracytoplasmic regions of these two proteins (~18% amino acid identity) breaks down almost completely prior to the last β strand in the crystal structure of FtsQ (Fig. 3 shows the sequence alignment). Moreover, the secondary structure of the β domain of *S. pneumoniae* DivIB, which can be reliably predicted from NMR-derived ^{13}C chemical shifts, is inconsistent with the final two β strands present in the FtsQ structure (25). Thus, it is conceivable that the C-terminal region of the DivIB β domain differs structurally from the corresponding region of FtsQ. However, we anticipate that this region of the β domain, which encompasses only ~20 residues, will be located in a topologically similar position in DivIB. Thus, we believe that the *E. coli* FtsQ structure provides a valid model for mapping the interaction of DivIB with FtsL, DivIC, and PBP 2B.

Figure 5A and B show molecular surface and ribbon representations of *E. coli* FtsQ, with the α and β domains highlighted in green and blue, respectively. The small γ tail, which is predicted to be unstructured (31), is shown schematically as a gray ribbon in Fig. 5B. Masson et al. (25) recently demonstrated a direct interaction between the β domain of DivIB and the FtsL-DivIC heterodimer and used NMR chemical shift mapping to pinpoint β domain residues that interact directly with the FtsL-DivIC heterodimer or are in close proximity to the interaction site. These residues are highlighted in red in Fig. 5A, and two points should be noted. First, these residues are largely restricted to a single face of the β domain, as evidenced by the two surface views related by a 180° rotation around the long axis of the molecule. Second, these residues are mostly, but not exclusively, restricted to the N-terminal end of the β domain (i.e., proximal to the α domain).

Masson et al. (25) proposed that these residues in the β domain of DivIB interact directly with the C-terminal regions of FtsL and DivIC. FtsL and DivIC are predicted to form a heterodimeric coiled coil comprising the bulk of their extracytoplasmic regions. However, it is their C-terminal 30 residues, which are not part of the coiled coil, that mediate their interaction with DivIB. Gonzalez et al. recently demonstrated that the C-terminal 22 residues of the 121-residue *E. coli* FtsL protein mediate its interaction with FtsQ (14), whereas residues 85 to 90 in the 103-residue FtsB protein from *E. coli* (i.e., the Gram-negative homolog of DivIC) are critical for its interaction with FtsQ (15). These results derived from *E. coli* are consistent with previous observations made using the orthologous *B. subtilis* proteins (20, 34), indicating that the mechanism of interaction between FtsQ and the FtsL-FtsB heterodimer is conserved in Gram-positive bacteria. Thus, in the model of the DivIB/PBP 2B/FtsL/DivIC complex shown in Fig. 5C, we show the extreme C-terminal regions of FtsL and DivIC interacting with the β domain of DivIB, as proposed by Masson et al. (25).

The primary contribution of the current work is that it has enabled a critical site of interaction between DivIB and PBP 2B to be mapped to a region immediately proximal to the site on DivIB that mediates its interaction with the FtsL-DivIC heterodimer. For the first time, this enables us to model the catalytic domain of PBP 2B in close proximity to the C-terminal regions of FtsL and DivIC. In Fig. 5A and B, the C-terminal region of the β domain that we determined to be critical for interaction with PBP 2B is shown in orange. This region (residues 229 to 257 in *B. subtilis* DivIB) corresponds to the final two strands of the elongated β sheet of the β domain in the crystal structure of *E. coli* FtsQ (although, as discussed above, the secondary structure of this region may be slightly different in DivIB and FtsQ). The A252P mutation that renders FtsQ incapable of recruiting FtsI (i.e., the *E. coli* ortholog of PBP 2B) is located within the corresponding region of FtsQ (13), suggesting that this mechanism of interaction between DivIB and PBP 2B is conserved across Gram-negative and Gram-positive bacteria.

No structures are available for PBP 2B, so in Fig. 5C we have used the crystal structure of PBP2x, an ortholog from *S. pneumoniae* (6, 26, 27), as a proxy for the structure of PBP 2B. The extracytoplasmic regions of these two transpeptidases are 33% identical, and the sequence alignment extends over all the entire length of PBP2x; thus, the PBP2x structure is likely a good surrogate for that of PBP 2B. PBP2x contains three

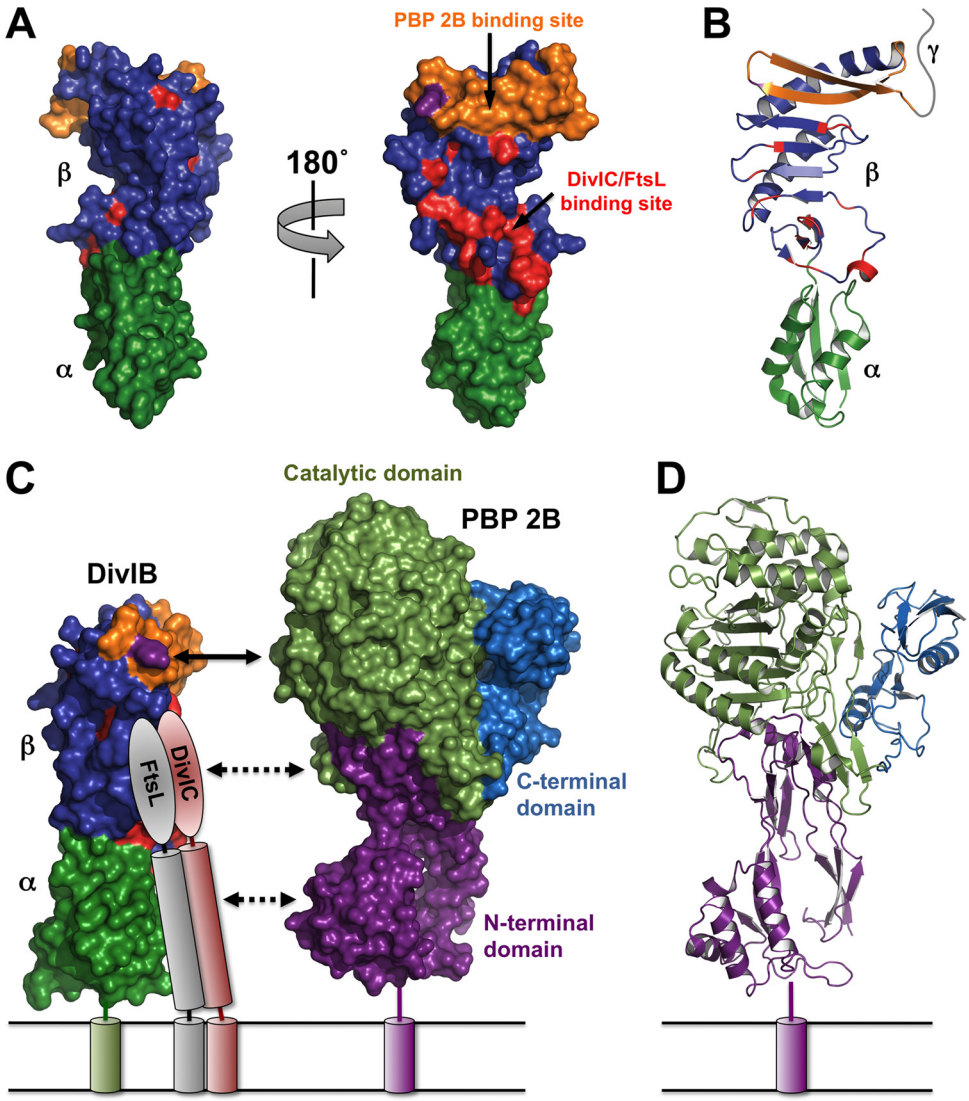

FIG. 5. (A) Surface representation of the crystal structure of *E. coli* FtsQ (Protein Data Bank [PDB] file 2VH1). The views on the left and right are related by a 180° rotation around the long axis of the molecule. The α and β domains are shown in dark green and blue, respectively. Residues previously demonstrated to be involved in the interaction of *S. pneumoniae* DivIB with the FtsL-DivIC heterodimer (25) are highlighted in red while the region shown in the current study to be critical for the interaction with PBP 2B (i.e., residues 229 to 257) is shown in orange. Note that these protein-protein interaction epitopes are mutually exclusive. The Y246 residue that leads to cell death at elevated growth temperatures when mutated to Ala is highlighted in magenta. (B) Ribbon representation of *E. coli* FtsQ highlighting the secondary structure of the regions involved in interaction with PBP 2B, FtsL, and DivIC. The color scheme and molecular orientation are the same as those of the molecule shown on the right in panel A. The highly variable γ tail is represented schematically as a gray ribbon. (C) Model of the DivIB/PBP 2B/FtsL/DivIC complex. The cytoplasmic domains and the γ tail of DivIB are omitted for the sake of clarity. The color scheme for DivIB is the same as in panels A and B. The C-terminal region and coiled-coil region of FtsL and DivIC are represented as ovals and cylinders, respectively. The C-terminal "heads" of the FtsL-DivIC heterodimer are shown interacting with residues in the β domain (red) that were defined by NMR chemical shift mapping (25). Shown to scale on the right is a surface representation of *S. pneumoniae* PBP2x. The region of DivIB demonstrated in the current study to be critical for interaction with PBP 2B (orange) aligns with the catalytic domain of PBP 2B (light green). The model suggests that the head and coiled-coil regions of the FtsL-DivIC heterodimer might interact with the transpeptidase and N-terminal domains of PBP 2B, respectively; these putative interactions are represented by the dotted lines. (D) Ribbon representation of the crystal structure of *S. pneumoniae* PBP2x with the N-terminal domain, catalytic domain, and C-terminal domain highlighted in magenta, light green, and cyan, respectively.

domains (Fig. 5D): (i) an N-terminal, membrane-proximal domain that has been proposed to be a regulatory domain, (ii) a central domain that encodes the transpeptidase activity, and (iii) a C-terminal domain of unknown function.

As shown in Fig. 5C, the region of DivIB that is critical for interaction with PBP 2B (orange) aligns with the middle of the central transpeptidase domain (light green) as well as the C-terminal domain of unknown function (blue). Since the latter domain is not conserved in Gram-negative divisomal transpeptidases such as FtsI, we suspect that this cannot be the site of interaction with DivIB. Rather, we predict that the C-terminal region of the β domain of DivIB makes contact with the catalytic transpeptidase domain of PBP 2B. Moreover, given the close proximity of the binding sites on DivIB for the C-terminal

regions of FtsL and DivIC, we predict that these regions also contact the transpeptidase domain of PBP 2B. This arrangement would also allow the coiled-coil regions of FtsL and DivIC to make contact with the membrane-proximal N-terminal domain of PBP 2B.

This new model strongly implicates the DivIB/FtsL/DivIC complex in regulating the transpeptidase activity of PBP 2B. This hypothesis is consistent with, and strongly supported by, many previous observations, including the following: (i) these three proteins are absent from bacteria without cell walls (14); (ii) *divIB* null cells form an abnormally thick cell wall during sporulation in *B. subtilis* (35), suggesting that the peptidoglycan cross-linking activity of PBP 2B is aberrant; (iii) extragenic suppressors of a *B. subtilis divIB* null strain map to the extracytoplasmic noncatalytic domain of PBP 2B (5), which is thought to modulate PBP 2B activity; (iv) increased expression of *divIB* in *B. subtilis* reduces the requirement for MurB, one of the enzymes in the biosynthetic pathway used to synthesize the key peptidoglycan precursor, lipid II (29); (v) deletion of *divIB* in *S. pneumoniae* leads to increased sensitivity to β-lactam antibiotics (19), which function by inactivating the transpeptidase activity of FtsI/PBP 2B (and other penicillin binding proteins).

Thus, the combined evidence strongly implicates the DivIB/FtsL/DivIC complex in regulating the synthesis of septal murein through its interaction with PBP 2B. This regulation of the enzymatic activity of PBP 2B could be of a positive or negative nature. It was recently suggested that *E. coli* FtsI is maintained in an inactive state in the divisome until inhibition is relieved through the subsequent recruitment of FtsN (4); moreover, it was shown in the same study that de-inhibition of FtsI is necessary for sensitivity to divisome-specific β-lactam antibiotics such as cephalexin. Thus, it is possible that the primary role of the DivIB/FtsL/DivIC complex is to act as a checkpoint which ensures that PBP 2B is maintained in an inactive state until an appropriate stage in the division cycle. This role would be consistent with the increased sensitivity of *S. pneumoniae* to β-lactam antibiotics when *divIB* is deleted (19).

In conclusion, we have shown that artificial septal targeting is a useful technique for examining the molecular details of pairwise interactions between divisomal proteins. By using this approach we were able to define a region on DivIB that is critical for its interaction with PBP 2B. The resultant model that we constructed of the DivIB/PBP 2B/FtsL/DivIC complex suggests that DivIB, DivIC, and FtsL play a role in regulating the transpeptidase activity of PBP 2B. Determination of the three-dimensional structure of the DivIB/PBP 2B/FtsL/DivIC complex is therefore likely to provide significant insight into the regulation of septal murein synthesis, as well as new avenues for the development of antibiotics that target bacterial cell division.

ACKNOWLEDGMENTS

This study was supported by project grant 519735 to G.F.K. from the Australian National Health and Medical Research Council and by an Institute for Molecular Bioscience Ph.D. scholarship to K.D.W.

REFERENCES

1. **Bi, E., and J. Lutkenhaus.** 1991. FtsZ ring structure associated with division in *Escherichia coli*. Nature **354:**161–164.
2. **Buddelmeijer, N., and J. Beckwith.** 2004. A complex of the *Escherichia coli* cell division proteins FtsL, FtsB and FtsQ forms independently of its localization to the septal region. Mol. Microbiol. **52:**1315–1327.
3. **Chen, J. C., M. Minev, and J. Beckwith.** 2002. Analysis of *ftsQ* mutant alleles in *Escherichia coli*: complementation, septal localization, and recruitment of downstream cell division proteins. J. Bacteriol. **184:**695–705.
4. **Chung, H. S., Z. Yao, N. W. Goehring, R. Kishony, J. Beckwith, and D. Kahne.** 2009. Rapid β-lactam-induced lysis requires successful assembly of the cell division machinery. Proc. Natl. Acad. Sci. U. S. A. **106:**21872–21877.
5. **Daniel, R. A., M. F. Noirot-Gros, P. Noirot, and J. Errington.** 2006. Multiple interactions between the transmembrane division proteins of *Bacillus subtilis* and the role of FtsL instability in divisome assembly. J. Bacteriol. **188:**7396–7404.
6. **Dessen, A., N. Mouz, E. Gordon, J. Hopkins, and O. Dideberg.** 2001. Crystal structure of PBP2x from a highly penicillin-resistant *Streptococcus pneumoniae* clinical isolate: a mosaic framework containing 83 mutations. J. Biol. Chem. **276:**45106–45112.
7. **Di Lallo, G., M. Fagioli, D. Barionovi, P. Ghelardini, and L. Paolozzi.** 2003. Use of a two-hybrid assay to study the assembly of a complex multicomponent protein machinery: bacterial septosome differentiation. Microbiology **149:**3353–3359.
8. **D'Ulisse, V., M. Fagioli, P. Ghelardini, and L. Paolozzi.** 2007. Three functional domains of the *Escherichia coli* FtsQ protein are involved in its interaction with the other division proteins. Microbiology **153:**124–138.
9. **Errington, J., R. A. Daniel, and D. J. Scheffers.** 2003. Cytokinesis in bacteria. Microbiol. Mol. Biol. Rev. **67:**52–65.
10. **Gamba, P., J. W. Veening, N. J. Saunders, L. W. Hamoen, and R. A. Daniel.** 2009. Two-step assembly dynamics of the *Bacillus subtilis* divisome. J. Bacteriol. **191:**4186–4194.
11. **Goehring, N. W., and J. Beckwith.** 2005. Diverse paths to midcell: assembly of the bacterial cell division machinery. Curr. Biol. **15:**R514–R526.
12. **Goehring, N. W., M. D. Gonzalez, and J. Beckwith.** 2006. Premature targeting of cell division proteins to midcell reveals hierarchies of protein interactions involved in divisome assembly. Mol. Microbiol. **61:**33–45.
13. **Goehring, N. W., I. Petrovska, D. Boyd, and J. Beckwith.** 2007. Mutants, suppressors, and wrinkled colonies: mutant alleles of the cell division gene *ftsQ* point to functional domains in FtsQ and a role for domain 1C of FtsA in divisome assembly. J. Bacteriol. **189:**633–645.
14. **Gonzalez, M. D., E. A. Akbay, D. Boyd, and J. Beckwith.** 2010. Multiple interaction domains in FtsL, a protein component of the widely conserved bacterial FtsLBQ cell division complex. J. Bacteriol. **192:**2757–2768.
15. **Gonzalez, M. D., and J. Beckwith.** 2009. Divisome under construction: distinct domains of the small membrane protein FtsB are necessary for interaction with multiple cell division proteins. J. Bacteriol. **191:**2815–2825.
16. **Grenga, L., G. Guglielmi, S. Melino, P. Ghelardini, and L. Paolozzi.** 10 May 2010. FtsQ interaction mutants: a way to identify new antibacterial targets. N. Biotechnol. doi:10.1016/j.nbt.2010.05.002.
17. **Harry, E. J., B. J. Stewart, and R. G. Wake.** 1993. Characterization of mutations in *divIB* of *Bacillus subtilis* and cellular localization of the DivIB protein. Mol. Microbiol. **7:**611–621.
18. **Karimova, G., N. Dautin, and D. Ladant.** 2005. Interaction network among *Escherichia coli* membrane proteins involved in cell division as revealed by bacterial two-hybrid analysis. J. Bacteriol. **187:**2233–2243.
19. **Le Gouëllec, A., L. Roux, D. Fadda, O. Massidda, T. Vernet, and A. Zapun.** 2008. Roles of pneumococcal DivIB in cell division. J. Bacteriol. **190:**4501–4511.
20. **Levin, P. A., and R. Losick.** 1994. Characterization of a cell division gene from *Bacillus subtilis* that is required for vegetative and sporulation septum formation. J. Bacteriol. **176:**1451–1459.
21. **Lewis, P. J., and A. L. Marston.** 1999. GFP vectors for controlled expression and dual labelling of protein fusions in *Bacillus subtilis*. Gene **227:**101–109.
22. **Lock, R. L., and E. J. Harry.** 2008. Cell-division inhibitors: new insights for future antibiotics. Nat. Rev. Drug Discov. **7:**324–338.
23. **Maggi, S., O. Massidda, G. Luzi, D. Fadda, L. Paolozzi, and P. Ghelardini.** 2008. Division protein interaction web: identification of a phylogenetically conserved common interactome between *Streptococcus pneumoniae* and *Escherichia coli*. Microbiology **154:**3042–3052.
24. **Margolin, W.** 2005. FtsZ and the division of prokarytotic cells and organelles. Nat. Rev. Mol. Cell Biol. **6:**862–871.
25. **Masson, S., T. Kern, A. Le Gouellec, C. Giustini, J. P. Simorre, P. Callow, T. Vernet, F. Gabel, and A. Zapun.** 2009. Central domain of DivIB caps the C-terminal regions of the FtsL/DivIC coiled-coil rod. J. Biol. Chem. **284:**27687–276700.
26. **Pares, S., N. Mouz, Y. Petillot, R. Hakenbeck, and O. Dideberg.** 1996. X-ray structure of *Streptococcus pneumoniae* PBP2x, a primary penicillin target enzyme. Nat. Struct. Biol. **3:**284–289.
27. **Pernot, L., L. Chesnel, A. Le Gouellec, J. Croize, T. Vernet, O. Dideberg, and A. Dessen.** 2004. A PBP2x from a clinical isolate of *Streptococcus pneumoniae* exhibits an alternative mechanism for reduction of susceptibility to β-lactam antibiotics. J. Biol. Chem. **279:**16463–16470.
28. **Piette, A., C. Fraipont, T. Den Blaauwen, M. E. Aarsman, S. Pastoret, and M. Nguyen-Disteche.** 2004. Structural determinants required to target peni-

cillin-binding protein 3 to the septum of *Escherichia coli*. J. Bacteriol. **186:** 6110–6117.
29. **Real, G., and A. O. Henriques.** 2006. Localization of the *Bacillus subtilis murB* gene within the *dcw* cluster is important for growth and sporulation. J. Bacteriol. **188:**1721–1732.
30. **Robichon, C., G. F. King, N. W. Goehring, and J. Beckwith.** 2008. Artificial septal targeting of *Bacillus subtilis* cell division proteins in *Escherichia coli*: an interspecies approach to the study of protein-protein interactions in multiprotein complexes. J. Bacteriol. **190:**6048–6059.
31. **Robson, S. A., and G. F. King.** 2006. Domain architecture and structure of the bacterial cell division protein DivIB. Proc. Natl. Acad. Sci. U. S. A. **103:**6700–6705.
32. **Robson, S. A., K. A. Michie, J. P. Mackay, E. Harry, and G. F. King.** 2002. The *Bacillus subtilis* cell division proteins FtsL and DivIC are intrinsically unstable and do not interact with one another in the absence of other septasomal components. Mol. Microbiol. **44:**663–674.
33. **Romberg, L., and P. A. Levin.** 2003. Assembly dynamics of the bacterial cell division protein FtsZ: poised at the edge of stability. Annu. Rev. Microbiol. **57:**125–154.
34. **Sievers, J., and J. Errington.** 2000. The *Bacillus subtilis* cell division protein FtsL localizes to sites of septation and interacts with DivIC. Mol. Microbiol. **36:**846–855.
35. **Thompson, L. S., P. L. Beech, G. Real, A. O. Henriques, and E. J. Harry.** 2006. Requirement for the cell division protein DivIB in polar cell division and engulfment during sporulation in *Bacillus subtilis*. J. Bacteriol. **188:**7677–7685.
36. **van den Ent, F., T. M. Vinkenvleugel, A. Ind, P. West, D. Veprintsev, N. Nanninga, T. den Blaauwen, and J. Löwe.** 2008. Structural and mutational analysis of the cell division protein FtsQ. Mol. Microbiol. **68:**110–123.
37. **Vicente, M., A. I. Rico, R. Martinez-Arteaga, and J. Mingorance.** 2006. Septum enlightenment: assembly of bacterial division proteins. J. Bacteriol. **188:**19–27.
38. **Wadsworth, K. D., S. L. Rowland, E. J. Harry, and G. F. King.** 2008. The divisomal protein DivIB contains multiple epitopes that mediate its recruitment to incipient division sites. Mol. Microbiol. **67:**1143–1155.
39. **Weiss, D. S.** 2004. Bacterial cell division and the septal ring. Mol. Microbiol. **54:**588–597.
40. **Weiss, D. S., J. C. Chen, J.-M. Ghigo, D. Boyd, and J. Beckwith.** 1999. Localization of FtsI (PBP3) to the septal ring requires its membrane anchor, the Z ring, FtsA, FtsQ, and FtsL. J. Bacteriol. **181:**508–520.
41. **Wissel, M. C., and D. S. Weiss.** 2004. Genetic analysis of the cell division protein FtsI (PBP3): amino acid substitutions that impair septal localization of FtsI and recruitment of FtsN. J. Bacteriol. **186:**490–502.
42. **Wissel, M. C., J. L. Wendt, C. J. Mitchell, and D. S. Weiss.** 2005. The transmembrane helix of the *Escherichia coli* division protein FtsI localizes to the septal ring. J. Bacteriol. **187:**320–328.